

We are IntechOpen, the world's leading publisher of Open Access books Built by scientists, for scientists

6,900

Open access books available

186,000

International authors and editors

200M

Downloads

Our authors are among the

154

Countries delivered to

TOP 1%

most cited scientists

12.2%

Contributors from top 500 universities



WEB OF SCIENCE™

Selection of our books indexed in the Book Citation Index
in Web of Science™ Core Collection (BKCI)

Interested in publishing with us?
Contact book.department@intechopen.com

Numbers displayed above are based on latest data collected.
For more information visit www.intechopen.com



Experimental Verification of Solidification Stress Theory

Charles Solbrig, Matthew Morrison and Kenneth Bateman
Idaho National Laboratory
USA

1. Introduction

Two Ceramic Waste Forms (CWFs) have been formed in this work without the benefit of an analysis tool that could stop large scale cracking that occurs during solidification. Both showed severe cracking. This chapter describes a new theory for a stress not modeled before, termed here, the solidification stress. This stress is set-into a glass or ceramic cylinder being formed during the time period of solidification. It is due to the temperature gradient existing during solidification. This stress is in addition to the normal thermal stress calculated in a solid due to a temperature gradient.

This chapter describes 1) how this stress can be controlled to prevent damage, 2) the methods available to measure this stress, and 3) the significant damage which occurred during the formation of the two large ceramic cylinder prototype high level nuclear waste forms, and 4) measurements made during CWF2 that verified the theory can predict the conditions under which cracking occurs.

This research program is being conducted to develop a crack-free ceramic waste form (CWF) to be used for long term encasement of fission products and actinides resulting from electrorefining of spent nuclear fuel. A crack-free waste form should have more resistance to leaching than one with many cracks. The fission products are deposited in electrorefiner electrolyte salt as a byproduct of the removal of uranium and actinides process during reprocessing of spent nuclear fuel. The encasement is accomplished by absorbing the radioactive salts into zeolite, mixing the zeolite-salt mixture with glass frit in a stainless steel cylindrical can, heating to a temperature range (600 °C) where consolidating and melting take place, then further heating up to a completely molten state at 915 °C causing the zeolite to convert to sodalite glass matrix, and then the sodalite glass matrix is solidified by cooling it through solidification (~625 °C), then further cooling to near ambient temperature. If cracking occurs which is usually the case, it will occur during the cooldown phase which is a detriment to long term encasement.

In this research, a model was developed that proposes a permanent stress develops, called solidification stress, when the melt solidifies and that this stress, if large enough, will cause failure as the CWF nears room temperature. This stress is proportional to the rate of cooling

during solidification. This stress is in addition to the thermal stress which develops during rapid cooldown of a solid. Two CWF's have been formed in this research, both of which encountered severe cracking. Sufficient data was recorded on the second to test the theory developed. Recording of temperatures and the cracking sounds during CWF2 cooldown shows that the cracking is from this newly recognized stress and not the thermal stress. The theory was provisionally verified on two small scale experiments and were reported on in Solbrig and Bateman, 2010. A third CWF formation is planned that is predicted by the theory to be crack free if the specification is followed.

The solidification stress is of opposite sign of the thermal stress and remains constant after solidification. Its derivation is reported on in Solbrig and Bateman (2010) and summarized in this chapter. The theory predicts that cracking of the CWF would occur at low temperatures if caused by solidification stress but at high temperatures (somewhat below the solidification temperature) if caused by thermal stress. To reduce solidification stress, the cooldown rate during solidification should be reduced. Recording cracking sounds confirm the existence of this solidification stress since cracking occurred during the low temperature phase of the cooldown. A cooldown rate history is proposed that should eliminate cracking in the next CWF formed.

CWF2 is a prototype vertical ceramic waste cylinder formed over a period of 10 days by heating a mixture of 75% zeolite, 25% glass frit in an argon atmosphere furnace through melting to 925 °C and then cooling through solidification to room temperature. It is approximately 1 m high, 0.5 m in diameter, weighs about 400 kg, and is formed in a stainless steel can 0.5 cm thick. This cylinder developed many cracks on cooldown. At least 15 loud cracks were recorded over a period of 4 days at the end of cooldown when the temperatures were below 400 °C, the last being after the CWF was removed from the furnace when the surface temperature was below 100 °C.

The CWF2 surface and centerline temperatures at mid height were recorded which allowed the stresses to be calculated. The timing of the cracks was compared to the time the calculated total stress exceeded the tensile stress limit and verified that the cause of the cracking was solidification stress and not thermal stress. Since the CWF is encased in a can in a furnace, the cracks cannot be easily observed but can be detected with sound measurements. Similarly, the stress cannot be measured but only estimated with analysis. Destructive examination of the CWF after cooldown was used to show the large amount of the cracking which occurred. It appeared to be initiated mainly in the inner region which is further evidence the cracking is due to solidification stress since solidification stress is tensile in the inner region and thermal stress is compressive in the inner region.

2. Theoretical background

The first part of this section describes some of the significant experimental work which has been reported on in the literature. The second part of this section summarizes the theory developed in this work which describes why the solidification stress is formed during solidification and how the solidification stress causes the CWF to form significant cracks near room temperature as they cool down.

2.1 Background experimental work

Faletti and Ethridge (1986) summarized the work done by several investigators who formed full-size waste form cylinders and supplied enough information for analysis of the results. The cylinder sizes were 50 to 60 cm in diameter and 150 to 300 cm in length and were either ceramic or glass. This is the size of the cylinders scheduled to be stored in U.S. Department of Energy (DOE) waste storage containers. Glass or ceramics have the characteristic of failing at their elastic limit. Due to nature of ceramics and glass, they crack to relieve tension instead of yield. Even though they are contained in a stainless steel can 0.5 cm thick, it is assumed that the can will rust away in a hundred years or so that the CWF will be exposed to the environment after this.

The Pacific Northwest Laboratories (PNL) report shows the cross section of a 60-cm-diam cylinder that illustrated considerable stress damage that occurred during cooling. The report goes on to state that all cylinders show similar damage during formation. One of the few known cases of crack-free waste forms were 15 cm (6 in.) formed by the continuous melt process, as indicated by Slate et al.(1978). Faletti and Ethridge (1986) state that cooling can proceed at any practical rate until the glass reaches its annealing point of 500 to 550 °C. Further cooling would have to proceed on the order of 1 °C/h implying nearly 3 weeks to cool a 60-cm-diam (24 in.) canister.

The formation of the cylinders reported on here is different than the PNL cylinders since the zeolite glass mixture consolidates as it heats up. A heavy weight is placed on the CWF as it heats up to compress it and keep voids from forming during consolidation. By the time it is ready for cooling, the zeolite has reacted to sodalite and has consolidated by a factor of more than 2.

2.2 Solidification stress model

For the convenience of the reader, the equation development from Solbrig and Bateman (2010) is summarized in this section. Only the axial stresses are modeled. The circumferential and axial stresses are equal on the circumference at the-plane so considering one of them is approximately equivalent to considering both. The radial stresses are small.

Thermal Stress: To understand the solidification stress model, it is first necessary to review how thermal stresses are modeled that are induced in a solid by a temperature distribution in a non prestressed cylindrical solid. This development is consistent with Timoshenko and Goodier (1970). Non prestressed means that there is no residual stress when the solid is at a uniform temperature. The cylinder is modeled as a series of concentric annuli. Each cylindrical annulus is intrinsically attached to the ones on either side of it. Each annulus temperature is uniform in the axial direction but the temperature of each is different in the radial direction. The length of the cylinder at any time is determined by length predicted using the Coefficient of thermal Expansion (CTE) based on the average temperature of the cylinder. Due to the intrinsic attachment of the annuli, the length of each is forced to be equal to the average length. Thus those annuli with temperatures above (T_{avg}) are forced to be shorter in length than their unattached thermally expanded length should be so they are in compression and those below T_{avg} are forced to be longer so are in tension.

Thus, the amount that annulus i must be elongated to reach the average length, L , is

$$\Delta L_i = L\alpha(T_{avg} - T_i)$$

where α = thermal expansion coefficient
 T_i = Temperature of annulus i

(1)

The stress, σ_i , induced in an annulus elongated by a length, ΔL_i , where a positive number signifies tension, is

$$\sigma_i = \frac{E}{1 - \mu} \frac{\Delta L_i}{L}$$

where E = Young's Modulus
 μ = Poisson's ratio

(2)

These two equations are combined to get the axial thermal stress at the mid-plane at any r as

$$\sigma_i = \frac{E\alpha}{1 - \mu}(T_{avg} - T_i)$$
(3)

This equation indicates that tensile stress in a cooling cylinder is largest at the surface. It should be noted that the circumferential surface stress is the same as the axial. So to get the magnitude of the total stress on the surface, this equation should be multiplied by the square root of two. For simplicity, in this chapter, the equivalent stress limit is applied in the axial direction only.

Solidification Stress is a Set-in Stress: A pre-stress is defined as a stress that exists when the temperature is uniform. A pre-stress induced by solidification is referred to here as a set-in stress. The total stress at any location is equal to the set-in stress plus the thermal stress. The stress which will cause the CWF to crack occurs during the cooldown. The cooling process starts from the highest temperature attained in the formation process at 925 °C where the CWF is all liquid and has no stress. As it is cooled, it eventually begins to effectively solidify at T_s (around 625 °C) where the viscosity becomes very large. During the cooling, the surface temperature is the lowest T because it is being cooled from the outside. Therefore, in terms of the model, the outside annulus solidifies first, then the second one in solidifies, followed by the third, etc. Each annulus is the same length when it solidifies $L(T_s)$. When the second annulus inward solidifies, the outer is shorter due to thermal contraction of the outside annulus as it has cooled below T_s . The two annuli are intrinsically connected along length $L(T_0)$ where T_0 is the temperature of the outer cylinder when the second one in inward solidifies. Therefore, these two cylinders are intimately connected along the length $L(T_0)$. The length not connected between these two annuli is defined here as the Length deficit, $L(T_s) - L(T_0)$.

As each successive cylinder solidifies, the solid one outward from it is shorter than it is. The length deficit for each annulus is the length not connected to the next outer annulus. When the whole cylinder reaches room temperature, the length deficits add up to form a dome shape. The dome height is larger with higher cooling rates. The length deficit causes a set-in stress when the temperature becomes uniform because all of the annuli are forced to be the same length. This stress is defined here as the solidification stress.

Figure 1 shows an exaggerated drawing of the total length deficit as a function of radius where the centerline total length deficit is shown at the left and the surface at the right.. The length deficits are small and would be difficult to see if the total annulus length were drawn instead of just the deficit. The total length deficit at any radius, r , is the sum of the individual length deficits from the outside and summing inward to radius, r . Each annulus is attached to the annulus on its inside but not along the length deficit.

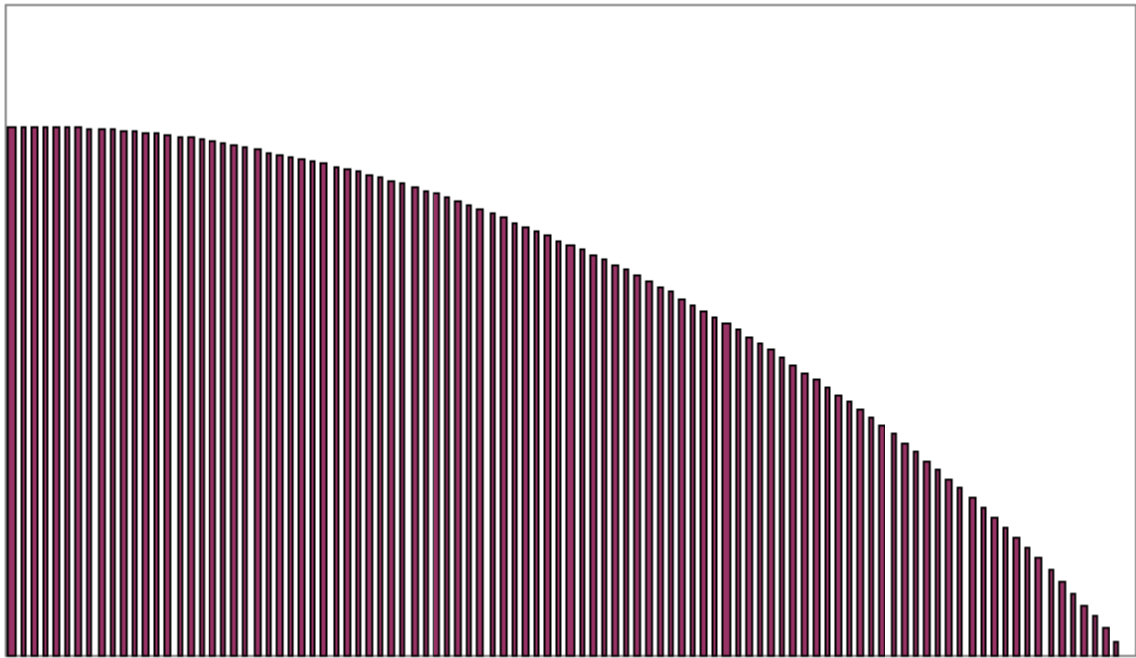


Fig. 1. Length Deficits.

The total length deficit at any r is

$$L_d = \int_{R_o}^r \frac{dL}{dr} \Big|_{s^+} dr \tag{4}$$

where the derivative is evaluated on the outer side of solidification front, s^+ , as the solidification front moves inward.

In a manner similar to the length deficit, a temperature deficit is defined as

$$\Delta T_i = T_s - T_{i+1} \tag{5}$$

where the annulus at r_i has just solidified, and T_{i+1} is the Temperature of the annulus at r_{i+1} at that time.

The total temperature deficit at any r is defined as

$$T_d = \int_{R_o}^r \frac{dT}{dr} \Big|_{s^+} dr \tag{6}$$

where the derivative is evaluated on the outer side of the solidification front, s^+ as the solidification front moves inward.

The temperature deficit is related to the length deficit by coefficient of thermal expansion as presented in equation 1. Substituting the length deficit into the equation for axial stress results in an equation for the set-in stress in terms of the temperature deficit distribution as:

$$\sigma_{\Delta l} = -\frac{E\alpha}{1-\mu}(\Delta T_{avg} - \Delta T_i) \quad (7)$$

The negative sign in front of the term on the right side of this equation is due to the fact that the change in the connective length is the negative of the change in the length deficit.

Note that both the thermal and solidification stresses are proportional to the CTE. Since the tensile stress at the failure limit is also calculated using the CTE, the stress limit is proportional to CTE as well.

3. Large scale experimental results – Verification of theory

CWF2 is a prototype vertical ceramic waste cylinder formed over a period of 10 days by heating a mixture of 75% zeolite, 25% glass frit in an argon atmosphere furnace through melting to 925 C and then cooling through solidification to room temperature. It is approximately 1 m high, 0.5 m in diameter, weighs about 400 kg, and is formed in a stainless steel can 0.5 cm thick. This cylinder developed many cracks on cooldown. At least 15 loud cracks were recorded over a period of 4 days at the end of cooldown when the temperatures had decreased below 400 C, the last occurred after the CWF was cool enough that it had been removed from the furnace. This section describes the results of this test.

3.1 Methods used to estimate stress

Stress cannot be measured during or after cooldown. Cracks cannot be visually observed as they occur because the CWF is encased in a stainless steel can and is in a furnace. Two methods used here to assess the stress: sound recordings and destructive examination. Although the cracking cannot be seen, the timing cracks can be detected with sound measurements. The CWF2 surface and centerline temperatures at mid height were measured which allowed the stresses caused by these temperature histories to be calculated using the theory. The timing of the cracks was compared to the time the calculated total stress exceeded the tensile stress limit and verified that the cause of the cracking was solidification stress and not thermal stress. So although the stress in the hot CWF cannot be measured, it can be estimated with the theory presented in this chapter. In order to know if the stress calculated will cause damage, it is necessary to know the failure limit. Subsection 3.2 discusses the tensile failure stress for the INL CWF and the method of measuring it. Subsection 3.3 presents the data obtained for the cracking sound recordings which were used to verify the theory. The next section (3.4) describes the temperature data that was used to estimate the stresses. Section 3.5 then presents the stresses calculated from these temperatures and determines the time of failure and

compares these times to the times at which cracking sounds were recorded. Destructive examination of the CWF after cooldown (described in Subsection 3.6) determined the location of cracking. It was initiated mainly in the inner region which is evidence the cracking is due to solidification stress.

3.2 Tensile stress limit measurements in CWF2

The tensile failure stress and the coefficient of thermal expansion (CTE) values in the above analysis have been estimated at 82.4 mpa (12000 psi) and $45 \times 10^{-6}/^{\circ}\text{C}$. The stress limit used is based experiments done on glass cylinders, Bateman and Solbrig (2008)a&b. The CTE was measured on CWF surrogates, Bateman and Capson (2003). The work described here is the first attempt to measure the tensile failure stress of the INL CWF and was made on CWF2 formed material. It was cut out of a piece removed from CWF2 at about the 1 foot high level. This region had cracked into many pieces during formation. The removed piece was a pie shaped wedge of 75 degrees, a radius of 25.4 cm (10 in), and a depth of about 0.94 cm (2.375 in.). A rectangular beam which was 0.34 cm (0.875 in) thick and 0.94 cm (2.375 in) wide was cut out of the wedge by the "A Core" Company. Due to the difficulty of cutting the material without breaking it, the beam was only about 8 inches long with uneven ends.

The method of determining the failure stress was to install the beam as a cantilever and apply a sufficient load on the cantilever to cause failure. In order to apply enough moment to reach the failure stress a metal extension was attached to the beam as shown in Figure 2.



Fig.2. Metal Extension attached to the CWF2 Beam

The exposed part of the CWF beam (about 2.54 cm ,1 in) was inserted into a vertically wall mounted vise as shown in Figure 3. The metal extension was 1.81 m (6 ft) long with a center of gravity of 0.9 m (3 ft) and clamped the CWF material to provide a cantilever. Weights were placed on the beam at the center of gravity (Figure 3). Weights were added until failure.



Fig.3. Weight placed on the beam 0.9 m (3 ft) from the vise

The first two pieces of the beam that broke off in the first two tests are shown in Figure 4. The longer one on the right was the first one broken off. The break planes were at about 5 degrees less than a 90 degree break.



Fig.4. Second (left) and First (right) Failed Sections

The maximum horizontal tensile stress for a given load can be calculated with an equation derived in Timoshenko and Mcaugh (1949). The stress calculated with the load at failure is the tensile failure stress limit. The maximum occurs at the top surface at the cantilever connection with the beam loaded at the end. The maximum tensile stress at the wall with the beam anchored as a cantilever is

$$\text{Stress} = \frac{Mc}{I}$$

where M = Total Moment about the cantilever support = $L * P$
 L = Length of the beam, P = total force on the end of the beam
 c = half the height of the beam = $h / 2$, h = height of the beam

$$I = \text{Vertical moment of inertia} = \frac{b * h^3}{12}, b = \text{width of beam}$$

(8)

Substituting the moment of inertia and moment into stress equation A.1 yields

$$\text{Stress} = \frac{6PL}{bh^2}$$

(9)

Three tests were run. The first three were successful and showed a range of values for failure tensile stress. The fourth may have been too short to get a realistic test. It seemed to crumble rather than break. The measurements are summarized in Table.1. The second and third tests are deemed to be the most accurate with the load reported for Test 2 being somewhat less than that which caused failure and the load for Test 3 being somewhat greater than the failure load. The accuracy of the load causing failure was limited by the use of discrete weights for the loading rather than a continuous loading device and the lack of additional samples to measure.

Date	Test	Failure load kg (lb)	Beam Weight kg (lb)	Total Load kg (lb)	Lever arm m (in)	Comment
6/21/10	1	4 (8.8)	1.36 (3)	5.36(11.8)	0.9(36)	First test.
6/22/10	2	6 (13.2)	1.36 (3)	7.36(16.2)	0.9(36)	Load <than failure
6/23/10	3	8 (17.6)	1.36 (3)	9.36(20.6)	0.9(36)	Load >than failure
6/24/10	4	2 (4.4)	1.36 (3)	3.36 (7.4)	0.9(36)	Crumbled, short

Table 1. Results of CWF2 Failure Measurements

The failure stress was calculated for the above experiments (Table.2). Neglecting the fourth test, the results show a failure yield stress of between between 9.66 mpa (1402 psi) and 16.9 mpa (2447 psi). The first test is a bit questionable, so a value of 15.2 mpa (2200 psi is reasonable. The last line was added to the table which shows that the beam would have had to support over 100 lbs to have a yield stress of 12000 psi. This is over 5 times as great as the loads which actually caused failure.

Test	Total Load kg (lb)	Failure Stress Mpa (psi)
1	5.36 (11.8)	9.6 (1402)
2	7.36 (16.2)	13.2 (1924)
3	9.36 (20.6)	16.9 (2447)
4	3.36 (7.4)	6.1 (879)
12 k Load	45.9 (101)	82.4 (12000)

Table 2. Failure Stresses Calculated for the Above Failure Loads

Thus, the testing has shown that the tensile yield stress of the sample removed from CWF2 is about 15.2 mpa (2200 psi). This is much lower than the 82.4 mpa (12000 psi) used in the model. However, the calculation of the stress is proportional to the Coefficient of Thermal Expansion. The CTE value used in the model is quite high for a ceramic, $45 \times 10^{-6} /C$, and was chosen in order to agree with measured data on contraction during cooldown, Bateman and Capson (2003).. It is the ratio of the CTE and the stress limit that is the actual criterion in determining failure. If the CTE is actually lower on the order of what is usual for a glass or ceramic of about $9 \times 10^{-6} /C$, then CWF2 would have failed when the total stress reached 16.5 mpa (2400 psi) which is close to the above measured value.

One other factor which should be considered is the actual state of the sample tested. It was taken from the outside region of the CWF which would have been in compression during cooldown before failure. There may have been fine cracks in the tested material because of all the damage which occurred. That is, the test may have been conducted on flawed material and perhaps a higher value would be obtained with a specimen from a CWF that does not crack during cooldown.

3.3 Sound recordings and timing of the cracking

A recording of the sound from the first crack recorded is shown in Figure 5. Time is plotted on the horizontal axis and proceeds from left to right. Sound power is plotted on the vertical axis. Background noise is recorded until the crack occurs evidenced by a large increase in power. The power then decreases exponentially back to the background level.

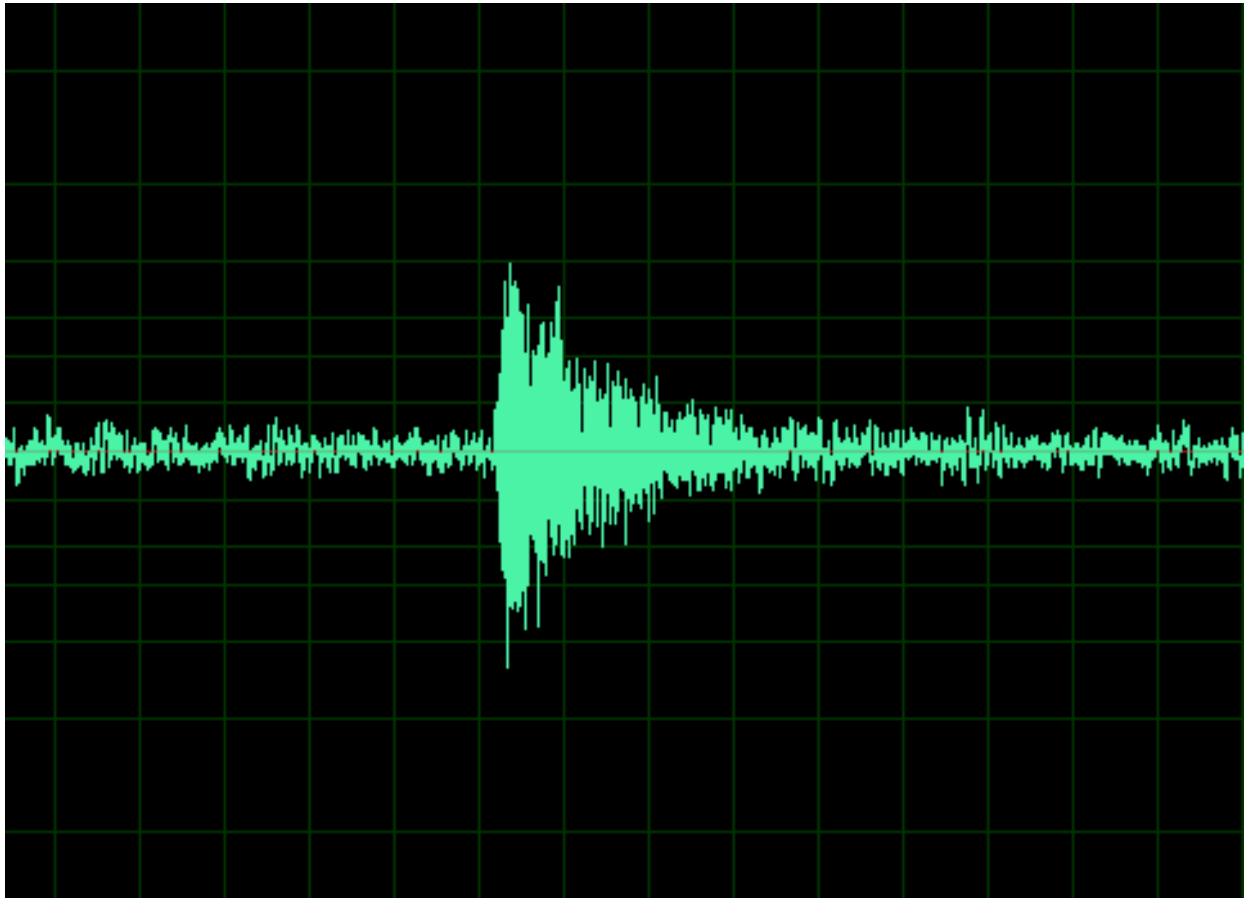


Fig.5.Sound Pressure of the First Crack Recorded.

All of the recordings looked similar but the power of the crack sound varied from crack to crack relative to the background noise. In general, the sound level decreased with each succeeding crack. The crack sounded like a loud gunshot even though the CWF was encased in a furnace with a insulating wall one foot thick. The total time duration in Figure 5 is about 2 seconds. The first crack occurred when the centerline temperature was 420 C and the surface temperature was about 400 C. Cracking continued down to near room temperature. The last crack occurred after the CWF had been removed from the furnace.

The timing of the cracks is included in Table B.1 along with the temperature data. The cracks do not occur at evenly spaced intervals. They usually occur several hours apart. The cracking analysis presented in this chapter applies to an uncracked cylinder and the cracking is probably relieving some of the stress. However, the theory predicts that the total stress continues to increase as the temperature decreases which explains why the cracking continues. The decrease of the sound power as cracking proceeds seems to indicate that

the stress in the remaining pieces is actually decreasing. The last crack occurred almost two days after the previous one and occurred after the CWF was removed from the furnace.

	Month/Day	Time	Hours since start.	Time between cracks	Sound level (db)*	Center-line Temperature of CWF (°C)**
Heat up	3/22	2:20 PM	0		NA	70
Cooldown	3/28	7:20 AM	137		NA	920
Crack 1	3/30	10:58 PM	200.6		91	420
Crack 2	3/31	1:28 AM	202.1	1.5	88	405
Crack 3	3/31	6:31 AM	208.2	6.1	91	382
Crack 4	3/31	3:11 PM	216.9	8.7	87	335
Crack 5	3/31	4:12 PM	217.9	1.0	85	325
Crack 6	4/01	12:55 AM	226.6	8.7	89	300
Crack 7	4/01	6:39 PM	244.3	17.7	81	220
Crack 8	4/01	7:49 PM	245.5	1.2	83	210
Crack 9	4/02	12:47 AM	250.5	5.0		190
Crack 10	4/02	2:11 AM	251.9	1.4		170
Crack 11	4/02	7:56 AM	257.6	5.8		150
Crack 12	4/02	10:39 AM	260.3	2.7		130
Crack 13	4/02	6:01 PM	267.7	7.4		110
Crack 14	4/03	10:57 AM	284.6	16.9		90
Crack 15	4/05	9:29 AM	331.2	46.5		70

* Sound level relative to a reference of 100 dB

**Temperatures estimated for Cracks 9 to 15

Table 3. Timing and Sound Levels of Cracking

3.4Temperature datafor CWF2

A cooling rate program was specified for the formation of CWF2 which was designed to eliminate cracking. This program was overridden by the protection program for the coolant blower so that severe cracking did occur. In the following section, the stress versus time in the CWF from the temperature data is estimated using the stress theory developed above. Then in a later section, the stress developed is compared to the stress limit and to the timing at which cracking occurred to demonstrate that not only does solidification stress exist but that it and not the thermal stress is responsible for cracking the CWF.

Surface and centerline temperatures were measured at the mid-plane. The surface mid-plane temperature history was then matched (by adjusting the heat transfer coefficients throughout the cooldown) in the CWF heat transfer, densification model developed in this work. Once this temperature history was matched with the code output, the temperature distributions in the solid were known. Then the stresses, thermal, solidification, and total, determined by the above equation could be calculated for the CWF. Then the cracking times were included on the stress plots. The cracking sounds all occurred when the calculated total stresses were above the stress limit. Although the thermal stress component exceeded

the stress limit early in the cooldown, cracking was not recorded during this time. When cracking occurred, the thermal stress was below the limit.

The mid-plane temperature measurements versus time made during the cooldown of CWF2 are shown in Figure 6. The centerline and surface temperatures are shown in this figure as well as the furnace wall temperature. In addition to the measured temperatures, the temperature history prescribed for the cooldown which should have kept the stress below the limit are shown. The measured rate of temperature drop (EXPerimental) through solidification is much more rapid than the desired (SPECification) curves. This results in a much larger temperature drop from the center to the surface than desired.

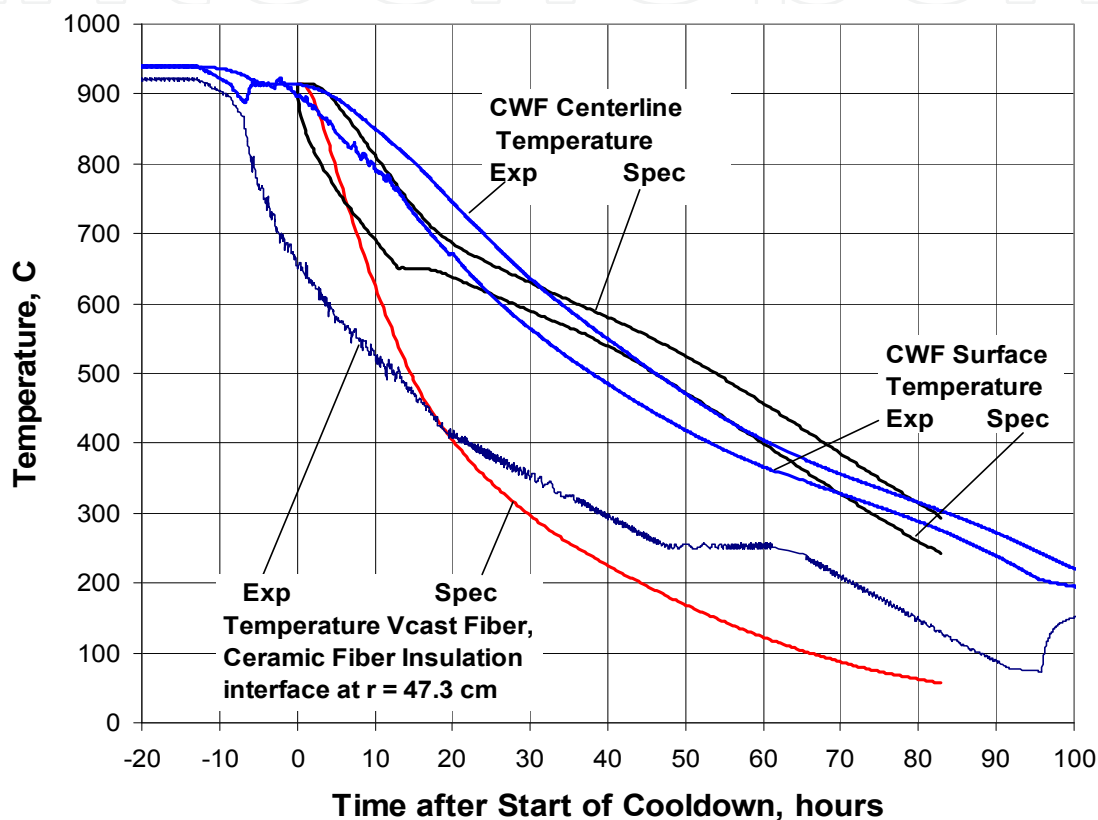


Fig.6.Experimental and Specification Temperatures at Mid-Plane

Note that the centerline temperature may be distinguished from the surface temperature since it is always greater than the surface temperature. The time scale in Figure 6 was adjusted so that zero time corresponds to the time that cooldown starts. It is 143 hours after the start of the initial heatup. The plan was to start cooldown 12 hours earlier. From Figure 6, it is seen that cooldown did start 12 hours earlier but after 4 hours the CWF cooldown and heat transfer from the CWF aborted, resulting in the surface and center temperatures equilibrating over the next hour. This was caused by the coolant blower tripping off due to a temperature limit (100 °C) being exceeded. It stayed off for about 8 hours but then the fan restarted so CWF cooldown started again (at zero time in Figure 6). The furnace wall continued cooling during the time that the fan was off because the control system kept the heating coils off. As temperatures decreased, the pump stayed on

for longer periods of time causing the average coolant flow to increase resulting in more heat being removed from the CWF. The largest heat removal occurred during solidification causing a large set-in stress.

To more clearly show the cooling rate problem encountered in CWF2, the temperature difference between the center and the surface is plotted in Figure 7. This difference during solidification is proportional to the solidification stress which is set-in.. The calculation specified that the temperature difference should decrease in the solidification range (about 625 C). The data shows the CWF2 temperature difference actually increased significantly.

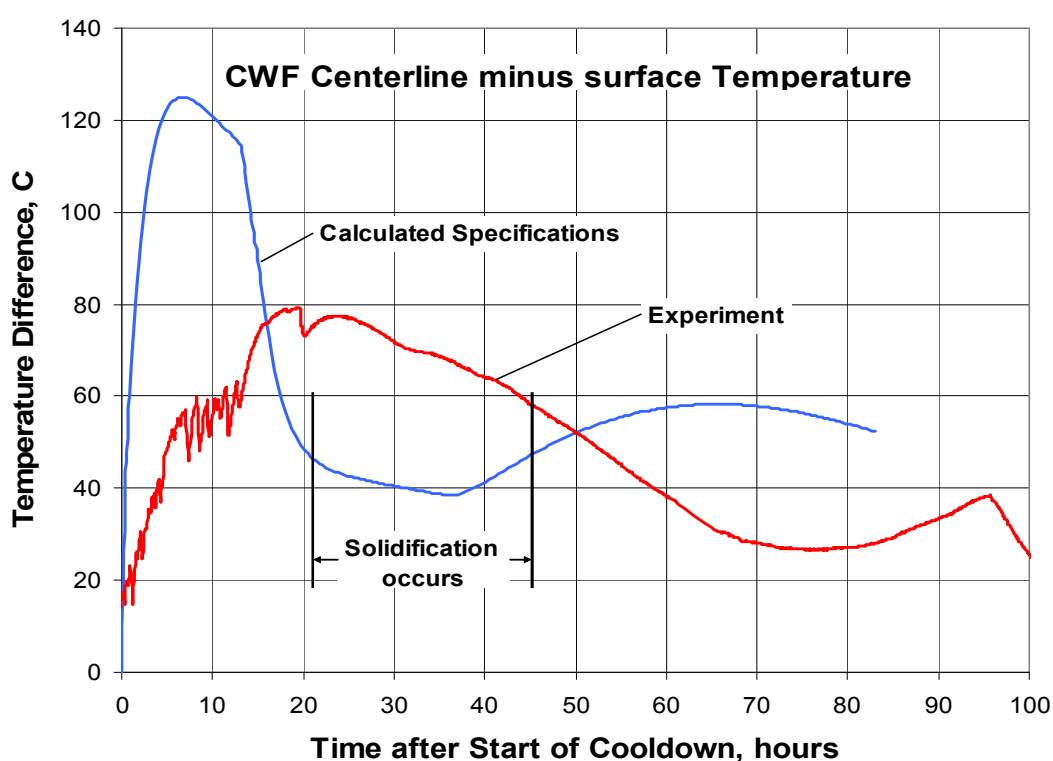


Fig.7. Temperature difference at Mid-Plane

In fact, the largest differences occur during solidification. The specification required the temperature difference to be less than 40 C but the data show it was nearly 80 C. This temperature difference resulted in CWF2 cracking. With the successful match of the surface temperature the other quantities of interest were available from the code. In particular, the centerline temperature, the radial temperature profile, and stresses developed, both solidification and thermal as well as total were available as code output. Figure 8 shows the agreement between the calculated temperatures on the surface and center of the CWF and the data. The calculations are a bit high in the CWF center (the higher temperature curve in Figure 8) at high temperature and a bit low at low temperature but the agreement is good in the important solidification region (between 725 C and 525 C). Below 300 C, the discrepancy between measured and calculated is not important because the thermal stress will continue to decrease and eventually the total stress will be just the solidification stress.

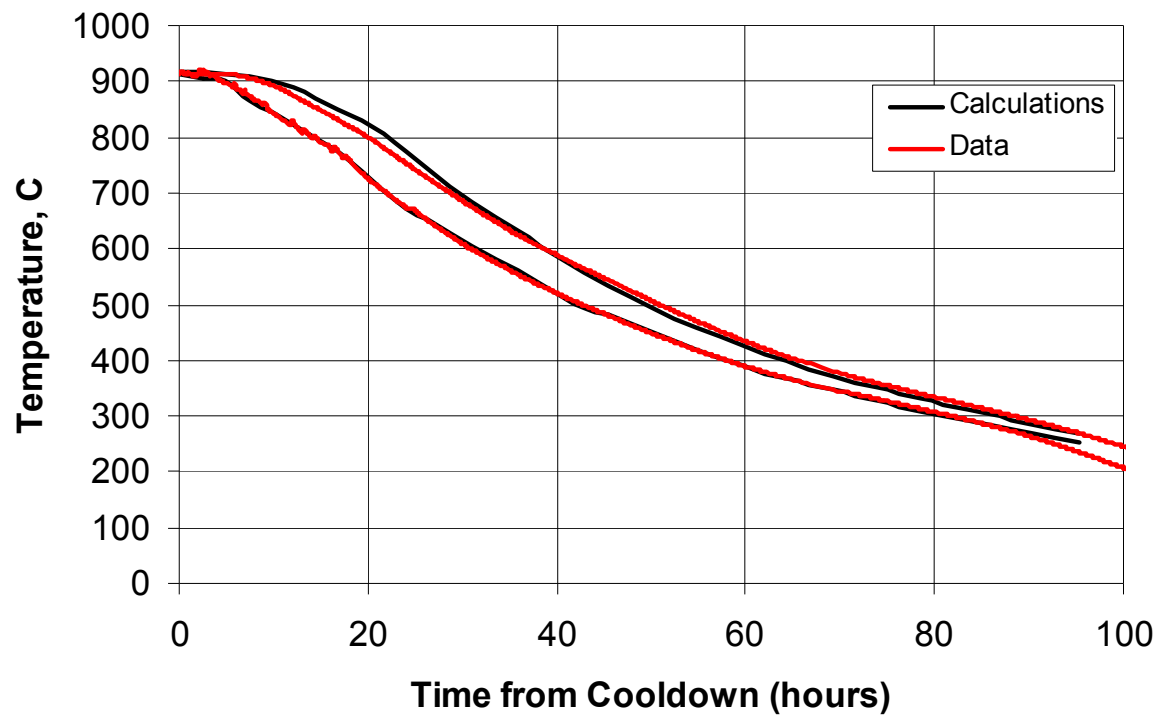


Fig.8. Comparison of Calculated Center and Surface Temperatures to Data (CWFformBig P01-CWF2.xls)

3.5 Comparison of calculated stress to the times cracking occurred

The next three figures show the thermal stress, the solidification stress and the total stress respectively output from the above mentioned code after the surface temperatures were matched. In each figure, the estimated tensile limit is included 82.4 mpa (12000 psi).

The thermal stress calculated through the mid-plane for this cooldown transient is shown in Figure 9. The stresses are shown at ten evenly spaced radial increments (spaced about 2.5 cm apart) with the center line stress being the largest negative value or compression and the outer surface being the largest positive value or tension. Thus, the thermal stress predicts that the stress will be in tension in the outer radial region of the CWF so that cracking would be expected to start in the outer radial region if solidification stress did not exist. In fact, the thermal stress at the outer radius is seen to exceed the tensile limit from 32 hours to 48 hours. The thermal stresses slowly decrease after that. If thermal stress were the cause of cracking in the CWF, it would be expected that cracking would occur during this time period. As mentioned sound measurements recorded 15 loud cracks during the course of the cooldown. The time of the first six cracks is indicated in the figure with numbers from 1 to 6. The first one occurred at 61 hours, much later than the 32 to 48 hours time interval when the thermal stress was above the tensile limit. Since all the cracks occurred significantly after the thermal stress reduced below the tensile limit, it cannot be responsible for the CWF damage. As mentioned previously only axial stresses are discussed in this chapter. Circumferential stresses are the same magnitude. Radial stresses are very small.

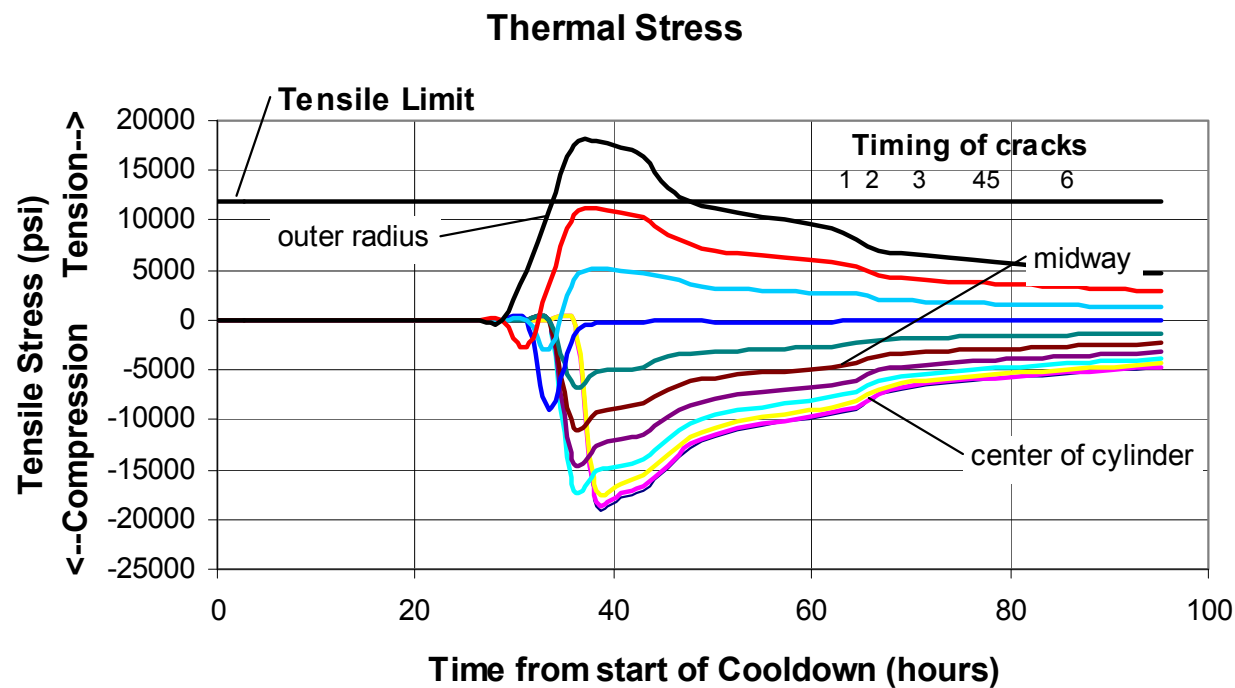


Fig.9. Thermal Stress at the mid-plane in the CWF (Note: 10000 psi=68.9 mpa)

Figure 10 shows the solidification stress calculated using the method developed in Solbrig and Bateman (2010) and summarized in the previous theory section. It develops while the CWF is solidifying and occurs because while one layer of the CWF is solidifying, it attaches itself to an adjacent solidified layer of a shorter length. As the solid then is cooled down to room temperature, all these different lengths are forced to the same length causing stresses.

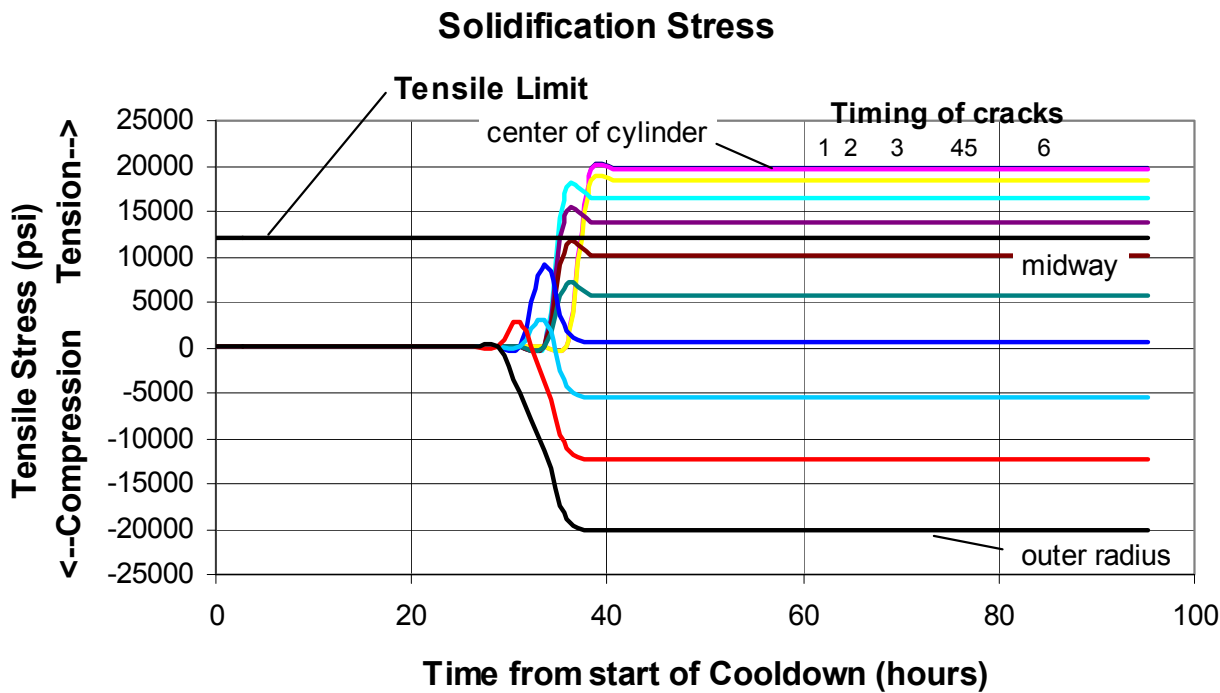


Fig.10. Solidification Stress of the CWF (Note: 10000 psi=68.9 mpa)

The solidification stress developed is dependent on the temperature profile during solidification but is independent of temperature profile during the remainder of the cooldown. Note that the solidification stress is of the opposite sign than the thermal stress and solidification stress and thermal stress subtract from each other.

Once the solidification stress develops, it is constant. The maximum solidification stress is about 137.9 mpa (20000 psi) which is well over the tensile stress limit of 82.4 mpa (12000 psi). The total stress is the sum of the thermal and the solidification stress, and since they are of opposite sign, the thermal stress partially cancels out the solidification stress especially during the early portion of cooldown in the solid phase. The thermal stress during the early period is responsible for keeping the total stress less than the tensile limit. But the thermal stress decreases as the temperature decreases, it cancels out less and less of the solidification stress as the temperature decreases and the temperature profile flattens out. When the temperature becomes uniform, the thermal stress is zero so the total stress is then equal to the 137.9 mpa (20000 psi) solidification stress at the cylinder surface at the mid-plane of the CWF. This explains why the CWF cracks at low temperature instead of high temperature where the thermal stress is high. That is, the combination of the solidification stress and the thermal stress results in the total stress continuing to increase as the average temperature decreases and the temperature profile flattens out and is highest when it is flat..

Both the solidification stress and the thermal stress are added together to obtain the total stress shown in Figure 11. The tensile total stress is zero out to 34 hours after the start of cooldown and then increases as the temperature decreases to room temperature.

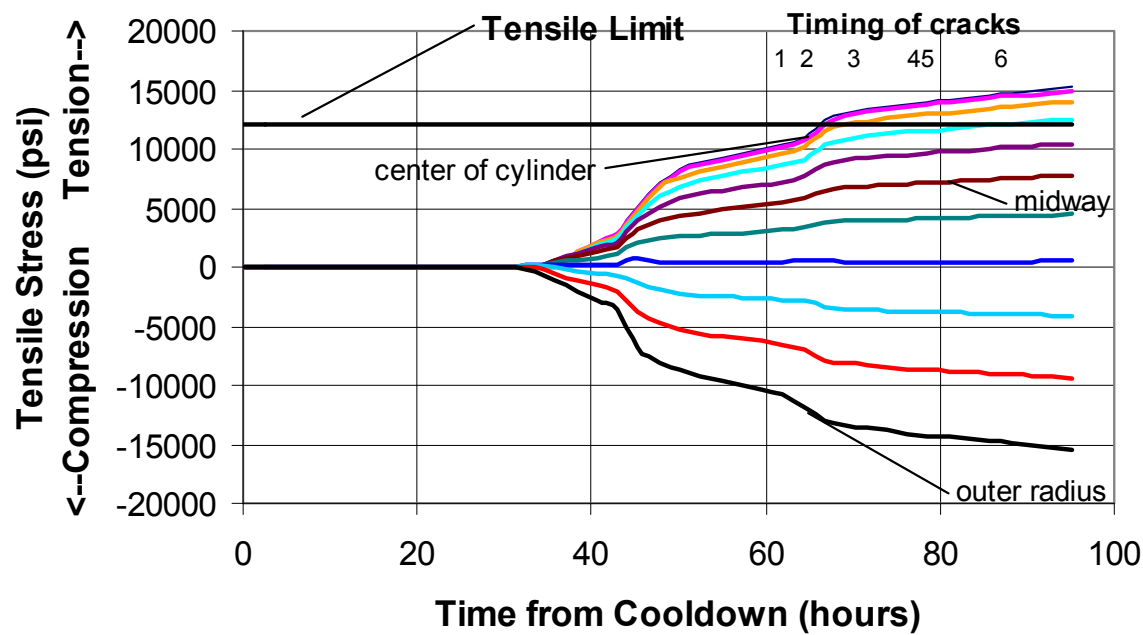


Fig.11. Total Stress of the CWF (Note: 10000 psi=68.9 mpa)

During the initial solidification period, the two stresses almost cancel each other out. The solidification stress is always greater than the thermal stress because the solidification temperature profile is always steeper than the temperature profile. Since the solidification stress is always in tension in the inner region, the total stress is also in tension in the inner portion of the cylinder. The total stress at the centerline eventually exceeds the tensile limit at 68 hours. The timing of the first six cracks is indicated by the upper numbers in Figure 11. The first cracking sound that was recorded occurred at 61 hours. This figure shows that the total surface stress is slightly less than the stress limit for the first two cracks but greater than the stress limit after that. The tensile limit shown is only an estimate and could be as low as 68.9 mpa (10000 psi). The damage continued all the way down to room temperature. In all, 15 loud cracks were heard including the last one which occurred after the CWF was at a low enough temperature that it was removed it from the furnace. Post test destructive examination of CWF2 confirmed the considerable damage which occurred.

It should be noted that if the temperature profile were to be flattened out at a high temperature, say 500 °C to ostensibly relieve stress, it would cause the CWF to crack at that temperature since the thermal stress would have been removed leaving the solidification stress to exceed the stress limit..

3.6 Visual confirmation of stress

Since it is not possible to measure the stress in the ceramic as it is forming, other means must be used to determine the stress which occurs during the formation. The timing of the sounds of cracking versus the calculated stresses is one method of estimating the stresses. Destructive examination of the resulting CWF is another. Since the CWF is formed in a steel canister, damage cannot be observed without destructive examination. Consequently, three one inch thick slices were cut out of both CWF1 and CWF2 with a 4 foot diameter diamond tipped saw blades. One slice was cut out at the mid section, another near the top, and a third near the bottom. In addition, an axial slice was cut through the center of the bottom half of CWF2. The cutting of the CWF did not seem to cause any of the cracking but the cracking occurred before the cutting. CWF2 was the first experiment that had sound recordings so similar measurements are not available for CWF1 but cracking seemed to occur in a similar manner as in CWF2..

Since CWF1 and CWF2 were run with the same cooldown cycle, damage to both were similar. Visual observation of CWF2 showed as much or more damage than CWF1. In addition, the axial cut of the lower half of CWF2 showed considerably more damage with parts of it appearing to be almost rubble.

The most egregious cracking which occurred in CWF1 is shown in Figure 12. This is a picture of the one inch thick slice cut out of the midsection of CWF1. Both axial and circumferential stress damage are observed in this picture. The pieces that have fallen out of the slice are caused by axial stress exceeding the stress limit in the axial direction. The radial cracks are due to the circumferential stress. Most of the damage occurs in the inner portion of the CWF confirming that the damage was caused solidification stress which is tensile in the inner region rather than thermal stress which is compressive in the inner region. Cracks in the circumferential direction are indications of radial stress. These appear in the outer region and may be caused by radial thermal stress.



Fig.12. Cracking in the mid-plane in CWF1

There is less damage to the one inch slices cut out of the top sections and bottom sections. This may be due to axial temperature gradients causing the highest solidification stresses to occur in axial middle portions of the CWF.

4. Conclusions

A theory has been developed to model a stress which was posited to develop when a ceramic solidifies due to the temperature gradient which exists during the solidification process. An experiment was run which verifies the existence of this stress. Thermal stress alone would have predicted cracking to occur while temperatures are high but when the solidification stress is added, the total stress calculation predicts cracking of the CWF will occur at low temperatures. Cracking sounds were recorded in this experiment and are used in this chapter to show that the existence of this stress is probable since cracking occurred during the low temperature phase of the cooldown. Confirmation of this model provides confidence in the ability of the model to predict a cooldown history for the next CWF formation which will eliminate cracking. Without including the solidification stress in the calculation, the low cooling rate needed to prevent cracking would be prescribed when thermal stress is high instead of during solidification and cracking would not be prevented with such a prescription.

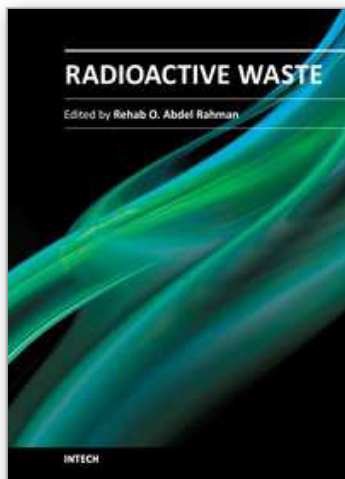
5. Acknowledgement

Work supported by the U.S. Department of Energy, Office of Nuclear Energy (NE) under DOE Idaho Operations Office Contract DE-AC07-05ID14517.

6. References

- Bateman, K. J. and Capson, D. D. (2003). "Consolidating Electrorefined Spent Nuclear Fuel Waste: Analysis and Experiment," *Proc. ASME Int. Mechanical Engineering Congress and Exposition (IMECE 2003)*, Washington, D.C., November 16–21, 2003. Figure 12.
- Bateman, K. J., and Solbrig, C.W. (2008)a. "Use of Similarity Analysis on Experiments of Different Size to Predict Critical Cooling Rates for Large Ceramic Waste Forms," *Proc. 16th Int. Conf. Nuclear Engineering (ICONE16)*, Orlando, Florida, May 11–15, 2008, American Society of Mechanical Engineers (2008).
- Bateman, K. J., and Solbrig, C.W. (2008)b. "Stabilizing Glass Bonded Waste Forms Containing Fission Products Separated from Spent Nuclear Fuel," *Sep. Sci. Technol.*, 43, 9, 2722 (July, 2008).
- Faletti, D. W., and Ethridge, L. J. (1986). "A Method for Predicting Cracking in Waste Glass Canisters," PNL 5947, Pacific Northwest Laboratories (Aug. 1986)
- Slate, S. C., Bunnell, L. R., Ross, W. A., Simonen, F. A., and Westsik, J. H. (1978). "Stress and Cracking in High-Level Waste Glass," PNL SA 7369, Pacific Northwest Laboratories, Dec. 1978.
- Solbrig, C. W., and Bateman, K. J. (2010). Modeling Solidification-Induced Stress in Ceramic Waste Forms Containing Nuclear Wastes, *Nuclear Technology*, Vol. 172, P 189-203, Nov, 2010.
- Timoshenko, S., and Goodier, J. N. (1970). *Theory of Elasticity*, Third Edition, McGraw-Hill, New York, NY (1970).
- Timoshenko, S., and MacCullough, G. H. (1949). "Elements of Strength of Materials," Van Nostrand, 3rd Ed., 1949, (P.122, Eq 49)

IntechOpen



Radioactive Waste

Edited by Dr. Rehab Abdel Rahman

ISBN 978-953-51-0551-0

Hard cover, 502 pages

Publisher InTech

Published online 25, April, 2012

Published in print edition April, 2012

The safe management of nuclear and radioactive wastes is a subject that has recently received considerable recognition due to the huge volume of accumulative wastes and the increased public awareness of the hazards of these wastes. This book aims to cover the practice and research efforts that are currently conducted to deal with the technical difficulties in different radioactive waste management activities and to introduce to the non-technical factors that can affect the management practice. The collective contribution of esteemed international experts has covered the science and technology of different management activities. The authors have introduced to the management system, illustrate how old management practices and radioactive accident can affect the environment and summarize the knowledge gained from current management practice and results of research efforts for using some innovative technologies in both pre-disposal and disposal activities.

How to reference

In order to correctly reference this scholarly work, feel free to copy and paste the following:

Charles Solbrig, Matthew Morrison and Kenneth Bateman (2012). Experimental Verification of Solidification Stress Theory, Radioactive Waste, Dr. Rehab Abdel Rahman (Ed.), ISBN: 978-953-51-0551-0, InTech, Available from: <http://www.intechopen.com/books/radioactive-waste/experimental-verification-of-solidification-stress-theory>

INTECH
open science | open minds

InTech Europe

University Campus STeP Ri
Slavka Krautzeka 83/A
51000 Rijeka, Croatia
Phone: +385 (51) 770 447
Fax: +385 (51) 686 166
www.intechopen.com

InTech China

Unit 405, Office Block, Hotel Equatorial Shanghai
No.65, Yan An Road (West), Shanghai, 200040, China
中国上海市延安西路65号上海国际贵都大饭店办公楼405单元
Phone: +86-21-62489820
Fax: +86-21-62489821

© 2012 The Author(s). Licensee IntechOpen. This is an open access article distributed under the terms of the [Creative Commons Attribution 3.0 License](https://creativecommons.org/licenses/by/3.0/), which permits unrestricted use, distribution, and reproduction in any medium, provided the original work is properly cited.

IntechOpen

IntechOpen